ELSEVIER

Journal of Nuclear Materials 277 (2000) 339–345

journal of nuclear materials

www.elsevier.nl/locate/jnucmat

Non-stoichiometry, electrical conductivity and defect structure of hyper-stoichiometric UO_{2+x} at 1000°C

Sun-Ho Kang[a], Jong-Ho Lee[a,1], Han-Ill Yoo[b,*], Han Soo Kim[c], Young Woo Lee[c]

[a] *Research Center for Thin Film Fabrication and Crystal Growing of Advanced Materials, Seoul National University, Seoul 151-742, South Korea*

[b] *School of Materials Science and Engineering, Solid State Ionics Research Laboratory, Seoul National University, Seoul 151-742, South Korea*

[c] *Korea Atomic Energy Research Institute, P.O. Box 105, Yuseong, Taejon 305-600, South Korea*

Received 9 January 1999; accepted 27 June 1999

Abstract

The oxygen non-stoichiometry (x) and electrical conductivity (σ) of hyper-stoichiometric UO_{2+x} have been measured as a function of partial pressure (P_{O_2}) at 1000°C by a solid-state coulometric titration technique and a dc 4-probe method, respectively. Both of the properties were found to be proportional to $P_{O_2}^{1/2}$ at the high oxygen partial pressure regime, and $P_{O_2}^{1/5}$ at the low oxygen partial pressure regime. These P_{O_2}-dependencies of the non-stoichiometry and the electrical conductivity are well explained with the (2:2:2) cluster model: $(2O_i^a 2O_i^b 2V_O)'$ and $(2O_i^a 2O_i^b 2V_O)''''$ are predominant at high and low P_{O_2}, respectively. The electron–hole mobility of UO_{2+x} at 1000°C has been determined by the combination of the non-stoichiometry and electrical conductivity combined on the basis of the (2:2:2) cluster model.

PACS: 07.07.-a; 28.52.Fa; 72.80.-r; 81.05.Je

1. Introduction

Thermodynamic and transport properties of uranium dioxide (UO_{2+x}) constitute a key issue in the application of the material for nuclear fuel since they are closely related to many chemical and physical processes during its use in the nuclear reactors, e.g., diffusion, creep, electrical and thermal conductivity, and release of fission products, which largely control the performance of the nuclear fuel during burnup [1,2].

Furthermore, these properties provide us an insight into the defect structure of the oxide. In the evaluation of the defect structure of a metal oxide, it is very useful and widely used to measure the thermodynamic and transport properties as a function of oxygen partial pressure, P_{O_2} at a fixed temperature. For example, non-stoichiometry (x) and electrical conductivity (σ) of a metal oxide are generally dependent on the oxygen partial pressure as $x \propto P_{O_2}^{1/m}$ and $\sigma \propto P_{O_2}^{1/n}$, and the defect structure of the metal oxide can be deduced from the oxygen exponents (m and n) by taking an appropriate defect model. The two oxygen exponents are not necessarily equal but complementary with each other through the electroneutrality condition. It is desirable, therefore, to measure both of the properties for the identical specimen to secure inter-consistency of the measured values in exploring the defect structure.

Up to now, the non-stoichiometry, electrical conductivity, and defect structure of UO_{2+x} have been studied by a number of investigators [3–13]. In spite of the numerous studies so far, however, agreements are rather poor among the reported results and the defect structure of UO_{2+x} has not been elucidated conclusively yet.

In the present work, the non-stoichiometry (x) and electrical conductivity (σ) of hyper-stoichiometric UO_{2+x} have been measured at 1000°C as a function of oxygen

* Corresponding author. Tel.: +82-2 880 7166; fax: +82-2 884 1413.

E-mail address: hiyoo@plaza.snu.ac.kr (H.-I. Yoo).

[1] Present address: Korea Institute of Science and Technology, Haweolgok 39-1, Seongbuk, Seoul 136-791, South Korea.

0022-3115/00/$ - see front matter
PII: S0022-3115(99)00155-5

partial pressure (P_{O_2}). From the two defect structure-sensitive properties the defect structure of hyper-stoichiometric UO_{2+x} is elucidated and compared with those reported by previous authors, and the mobility of electron–holes is determined by combining the non-stoichiometry and electrical conductivity.

2. Experimental

2.1. Sample preparation

UO_2 powder was prepared by the ammonium uranyl carbonate (AUC) conversion process and pressed at 300MPa into green pellets about 10mm in diameter and 10mm in length. The important impurities levels of the UO_2 powder are shown in Table 1. The green pellets were sintered at 1700°C for 4 h in hydrogen atmosphere in a tubular furnace, and the sintered UO_2 pellets were then crushed into small fragments for coulometric titration and cut into parallelepipeds (ca. 1.8 mm × 1.9 mm × 8.4 mm) for electrical conductivity measurement. Density of the sintered pellets measured by a water immersion method was 97.2% of the theoretical density.

2.2. Measurement of non-stoichiometry

Non-stoichiometry (x) of UO_{2+x} was measured by means of a solid-state coulometric titration technique with a high-temperature electrochemical cell,

$$\text{Pt, } UO_{2+x} | \text{ YSZ } | P_{O_2}^{\text{ref}}, \text{ Pt.}$$

The titration cell is schematically shown in Fig. 1. A disk of 8 mol% yttria-stabilized zirconia (8YSZ), 12.5 mm in diameter × (1–1.5) mm thickness, was employed as the solid electrolyte (#7 in the figure). For the purpose of gas-tight seal, silicate glass powder with a composition of 49 wt% SiO_2, 25 wt% BaO, 16 wt% B_2O_3, and 10 wt% Al_2O_3 was used (#8). At high temperatures above 1000°C, the silicate glass powder melts to provide a satisfactory gas-tight seal. Details of the preparation of the electrochemical cell have been described elsewhere [14,15].

Table 1
Impurities of UO_2 powder prepared by the AUC conversion process

Element	U (μg/g)	Elements	μg/g-U
Al	< 10	B	< 0.2
C	20	Ca	< 20
Cd	< 0.2	Cr	< 10
Cu	< 10	Dy	< 0.1
F	< 2	Fe	< 50
Gd	< 0.1	Mg	< 10
Mn	< 5	Mo	< 1
Ni	< 10	Si	< 10
Th	< 200		

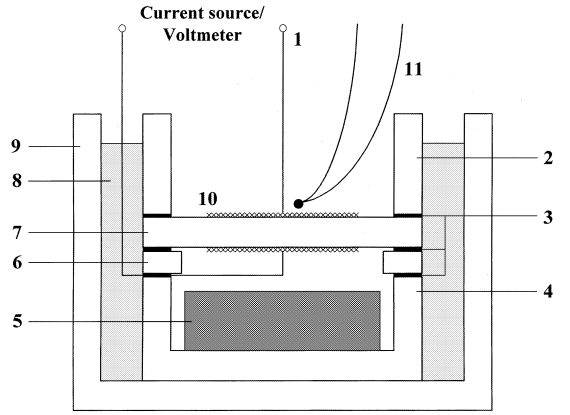

Fig. 1. Schematic diagram of the coulometric titration cell. (1) Pt–lead wire; (2) YSZ ring; (3) Pt-foil; (4) alumina cup; (5) UO_{2+x} specimen; (6) alumina ring; (7) YSZ disk; (8) silicate glass; (9) alumina crucible; (10) Pt-gauze; (11) S-type thermocouple.

Coulometric titration was performed by passing constant currents through the YSZ electrolyte with a dc current source (Keithley 224) and measuring the steady-state open-cell voltage across the electrolyte with a digital multimeter (Keithley 2000). The applied current was of the order of 100 μA. The amount of atomic oxygen, ΔN_O, which was removed from or added to the sample chamber can be calculated as

$$\Delta N_O = \frac{I\,t}{2F}, \tag{1}$$

where I and F denote the applied current for a time duration t and the Faraday constant, respectively. If the oxygen content in the dead volume of the sample chamber can be neglected, the change of the oxygen non-stoichiometry, Δx, in UO_{2+x} is then given as

$$\Delta x = x - x^* \approx \frac{M}{m}\Delta N_O = \frac{M\,I\,t}{2mF}, \tag{2}$$

where x^* is the non-stoichiometry at the starting point of coulometric titration, M the molar weight of the specimen, and m the specimen weight. After the current was turned off, the equilibrium oxygen partial pressure over the specimen, P_{O_2} has been determined via the Nernst equation

$$P_{O_2} = P_{O_2}^{\text{ref}} \exp(-4FE/RT), \tag{3}$$

where E is the steady-state open-cell voltage across the solid electrolyte, and $P_{O_2}^{\text{ref}}$ the oxygen partial pressure of the reference gas flowing outside the titration cell. In the present work, Ar/O_2 or CO_2/CO mixtures were em-

ployed as the reference gas, whose oxygen partial pressure, $P_{O_2}^{ref}$ was monitored with a stabilized zirconia oxygen concentration cell.

2.3. Measurement of electrical conductivity

The electrical conductivity (σ) was measured at 1000°C as a function of oxygen partial pressure by the conventional dc 4-probe method [16–18] as depicted in Fig. 2. Four pieces of Pt wire (2 as voltage probes and the others as current probes) were attached by twist-tightening around the specimens. By applying constant currents (I) through the two outer Pt-probes and measuring voltage drops (V) across the two inner Pt-probes, the electrical conductivity (σ) was calculated from the slope of the I–V curve by using the equation

$$V = \frac{L}{A}\frac{1}{\sigma} I, \tag{4}$$

where L and A are the distance between the two inner Pt-probes and the cross-sectional area, respectively. The current was varied in the range from −3.5 mA to +3.5 mA stepwise with 0.5 mA interval and the I–V curve showed a good linearity (the linear correlation coefficient, $R^2 > 0.99999$). The oxygen partial pressure was controlled by flowing CO_2/CO mixture gas and monitored with the same type of stabilized zirconia concentration cell as in the non-stoichiometry measurement.

3. Results and discussion

3.1. Non-stoichiometry

The oxygen partial pressure dependence of the non-stoichiometry of hyper-stoichiometric UO_{2+x} at 1000°C is shown in Fig. 3 together with the reported results by various authors via other methods than coulometric titration, e.g., thermogravimetry, E.M.F. measurement, and quenching technique [3–9].

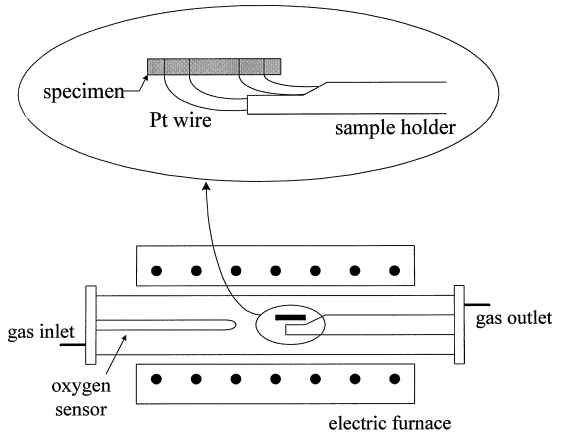

Fig. 2. Experimental set-up for the conductivity measurement.

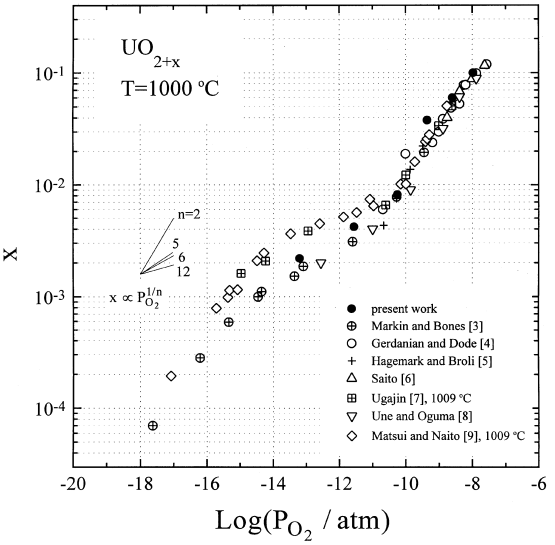

Fig. 3. Non-stoichiometry, x of hyper-stoichiometric UO_{2+x} at 1000°C as a function of oxygen partial pressure (P_{O_2}).

At the non-stoichiometry values (x) larger than about 0.006, all of the data are in fairly good agreement and the non-stoichiometry varies with the oxygen partial pressure as $x \propto P_{O_2}^{1/2}$. This oxygen partial pressure dependence of x may be explained with the defect cluster involving two kinds of interstitial oxygen (O_i^a and O_i^b) and oxygen vacancy, i.e., $(2O_i^a 2O_i^b 2V_O)$ cluster proposed by Willis [19] on the basis of neutron diffraction. Using the Kröger–Vink notation, the formation of this (2 : 2 : 2) cluster is represented by

$$2O_O^{\times} + O_2(g) + nU_U^x = (2O_i^a 2O_i^b 2V_O)^{n'} + nU_U^{\bullet}, \tag{5}$$

where n is the effective charge of the (2 : 2 : 2) cluster. From the following electroneutrality condition and site balance, respectively,

$$n[(2O_i^a 2O_i^b 2V_O)^{n'}] = [U_U^{\bullet}], \tag{6}$$

$$2[(2O_i^a 2O_i^b 2V_O)^{n'}] = x, \tag{7}$$

it can be easily shown that the non-stoichiometry is dependent on the oxygen partial pressure

$$x \propto P_{O_2}^{1/(n+1)}. \tag{8}$$

In Eqs. (6) and (7), the square brackets denote the number of corresponding structure elements per lattice molecule (1 UO_2 unit). Comparison of the experimental results with Eq. (8) gives us the effective charge of the (2 : 2 : 2) cluster and, consequently, in the high P_{O_2} regime of hyper-stoichiometric UO_{2+x} a singly ionized

$(2O_i^a 2O_i^b V_O)'$ cluster is concluded to be prevailing. The same defect structure of the oxide has been proposed at high P_{O_2} by Une and Oguma [8] at 1000°C, Matsui and Naito [9] at 1009°C, and Kim et al. [20] at 1200°C.

In the range of the non-stoichiometry, $0.001 < x < 0.006$, however, discrepancies are observed among the data as depicted in Fig. 3. In this region, which will be referred to as an intermediate P_{O_2} region, the non-stoichiometry obtained in this work as well as reported by Markin and Bones [3] and Une and Oguma [8] are found to be dependent on the oxygen partial pressure as $x \propto P_{O_2}^{1/5}$. This P_{O_2}-dependence of the non-stoichiometry may be explained with a quadruply ionized $(2O_i^a 2O_i^b 2V_O)''''$ cluster [i.e., $n=4$ in Eq. (8)]. Une and Oguma [8] also ascribed the non-stoichiometry variation in this region to the (2 : 2 : 2) cluster with effective charge of −4. Matsui and Naito [9], on the other hand, reported that the slope of log x vs. log P_{O_2} plot was 1/12 in the intermediate P_{O_2} region. To explain the 1/12-slope, they considered another kind of defect cluster involving more oxygen vacancies than the (2 : 2 : 2) cluster as follows:

$$2O_O^{\times} + \frac{1}{2}O_2(g) + nU_U^{\times} = (2O_i^a O_i^b 2V_O)^{n'} + nU_U^{\bullet}. \qquad (9)$$

Electroneutrality condition and site balance yield the P_{O_2}-dependence of x as $x \propto P_{O_2}^{1/2(n+1)}$, and Matsui and Naito interpreted their results with $(2O_i^a O_i^b 2V_O)^{5'}$ cluster model. However, such a high ionized state of the (2 : 1 : 2) cluster seems to be energetically unstable as pointed out by Nakamura and Fujino [1]. Because the normal effective charge of the (2 : 1 : 2) cluster is −2, the $(2O_i^a O_i^b 2V_O)^{5'}$ cluster is considered as the $(2O_i^a O_i^b 2V_O)''$ cluster trapping 3 electrons. But since p-type conduction is predominant in this regime, as will be shown in the next section, it is less likely for the (2 : 1 : 2) cluster to be associated with electrons which are minority electronic defects. Furthermore, a closer examination reveals that the slope of Matsui and Naito's data in the intermediate P_{O_2} region is steeper than the 1/12-slope. Nakamura and Fujino [1], in their paper on the thermodynamic analysis of UO_{2+x} with the literature data, showed the possibility of $x \propto P_{O_2}^{1/(6-8)}$ in the intermediate P_{O_2} region and the dependence of x on the oxygen partial pressure might be explained with doubly ionized $(2:1:2)''$ cluster as a limiting case (i.e., $x \propto P_{O_2}^{1/6}$). As discussed so far, the defect structure in the intermediate P_{O_2} region has not been clarified conclusively. To ascertain it more reliably, other defect structure-sensitive properties, e.g., electrical conductivity, are required to be measured, which will be dealt with in the next section.

A few data are available in the near-stoichiometric composition in the low P_{O_2} region. Because the non-stoichiometry was not measured in this region in the present work, the defect structure will be discussed only with the literature data obtained by Markin and Bones [3], and Matsui and Naito [9]. In the low P_{O_2} region, a rise in the slope of log x − log P_{O_2} is observed and $x \propto P_{O_2}^{1/2}$ holds again as shown in Fig. 3. Matsui and Naito [9] attributed it to the neutral (2 : 1 : 2) cluster [i.e., $(2O_i^a O_i^b 2V_O)^{\times}$], which is contradictory from a defect chemical point of view. When two types of defects different only in the charge state are predominant in the neighboring P_{O_2} regimes, the defect with higher oxidation state should be prevailing at the higher P_{O_2} regime. In this sense, Matsui and Naito's analysis is reversed [$(2O_i^a O_i^b 2V_O)^{5'}$ cluster at the intermediate P_{O_2} region and $(2O_i^a O_i^b 2V_O)^{\times}$ cluster at the low P_{O_2} region]. With the non-stoichiometry data measured by Matsui and Naito [9], Nakamura and Fujino [1] proposed $(2O_i^a O_i^b 2V_O)''$ to be valid down to the near-stoichiometric composition. In fact, because the electronic disorder becomes predominant and the electroneutrality condition is $[e'] = [h^{\bullet}]$ in the low P_{O_2} region, any type of defect can explain the 1/2-slope if one mole of the defect is generated by incorporation of a half mole of oxygen molecule (i.e., $1/2O_2$). Considering a small extent of defect concentration at near-stoichiometric composition, one may also postulate an isolated oxygen interstitial (O_i'') as a major defect.

3.2. Electrical conductivity

The isothermal variation of the electrical conductivity (σ) of hyper-stoichiometric UO_{2+x} as a function of oxygen partial pressure at 1000°C is shown in Fig. 4 together with the literature data measured near 1000°C [10–13]. All of the conductivity data in Fig. 4 indicate that p-type

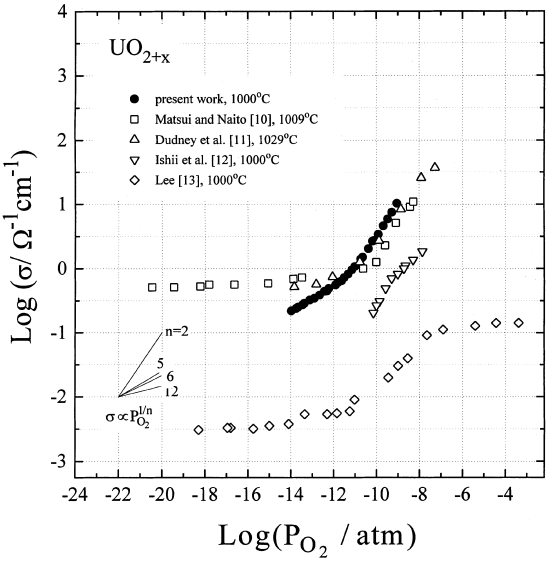

Fig. 4. Electrical conductivity, σ of hyper-stoichiometric UO_{2+x} at 1000°C as a function of oxygen partial pressure (P_{O_2}).

conduction prevails in the entire P_{O_2} range examined, i.e., the conductivity increases with increasing P_{O_2}. However, it is seen that there exist large disagreements in the magnitude of the conductivity among the data in Fig. 4 although the measurements of Refs. [10,11] were made at a little higher temperatures. For example, the electrical conductivity obtained in this work is about two orders higher than that reported by Lee [13].

Concerned with the P_{O_2}-dependence, the conductivity data obtained in this work including those reported by Matsui and Naito [10], and Dudney et al. [11] are dependent on the oxygen partial pressure to a half power, i.e., $\sigma \propto P_{O_2}^{1/2}$ at high P_{O_2}. Ishii et al.'s data [12] exhibit slight curvature, but due to the lack of the data at lower P_{O_2} it is not clear whether the curvature is significant or originated from experimental errors. If the curvature is ignored, one can say that the electrical conductivity reported by Ishii et al. also changes with the oxygen partial pressure as $\sigma \propto P_{O_2}^{1/2}$. The same feature was found for the non-stoichiometry as discussed in the previous section (i.e., $x \propto P_{O_2}^{1/2}$), which is readily expected from the following relations:

$$\sigma = c_h q \mu_h \tag{10}$$

and

$$c_h = \frac{4[U_U^\bullet]}{a_0^3} = \frac{4n[(2O_i^a 2O_i^b 2V_O)^n]}{a_0^3} = \frac{2n}{a_0^3}x, \tag{11}$$

where c_h denotes the concentration of electron–holes per lattice molecule, q the elementary charge, μ_h the mobility of electron–holes, and a_0 the lattice constant of UO_{2+x}. Consequently, the electrical conductivity supports the conclusion that the singly ionized $(2O_i^a 2O_i^b 2V_O)'$ cluster is prevailing in the high P_{O_2} region, which was drawn from the non-stoichiometry data. The conductivity data reported by Lee [13], however, show a different P_{O_2}-dependence at the high P_{O_2} region. Although Lee insisted that the oxygen partial pressure dependence of σ might be expressed as $\sigma \propto P_{O_2}^{1/2}$ in the range of $-11 \leqslant \log(P_{O_2}/\text{atm}) \leqslant -7$[13], it seems that the conductivity varies against the oxygen partial pressure as $\sigma \propto P_{O_2}^{1/3}$. At higher P_{O_2} than 10^{-7} atm, the conductivity is virtually independent of P_{O_2}, which may be ascribed to the formation of a second phase, e.g., U_4O_9, as was pointed out by Lee [13]. According to Nakamura and Fujino [21], the phase boundary of UO_{2+x}/U_4O_9 is located at $\log(P_{O_2}/\text{atm}) \cong -6$.

In the intermediate P_{O_2} region, the electrical conductivity obtained in this work shows the same oxygen partial pressure dependence as the non-stoichiometry of the present work, i.e., $\sigma \propto P_{O_2}^{1/5}$. This strongly supports the inter-consistency between the non-stoichiometry and electrical conductivity measured in this investigation, and the two results suggest that the quadruply ionized $(2O_i^a 2O_i^b 2V_O)''''$ cluster is predominant in the intermediate P_{O_2} region. However, Matsui and Naito's data exhibit a different trend from the present one. They reported that the conductivity revealed a 1/12-slope as in the case for the non-stoichiometry measured by them and explained the slope with the (2 : 1 : 2) cluster with effective charge of -5.

At the low P_{O_2} region, where the electrical conductivity has not been measured in the present study, the conductivity data reported by Matsui and Naito at 1009°C [10] and Lee at 1000°C [13] show no dependence on the oxygen partial pressure, which is because electron–holes are compensated by electrons, i.e., $[e'] = [h^\bullet]$.

3.3. Defect structure of hyper-stoichiometric UO_{2+x} at 1000°C

The defect structure of hyper-stoichiometric UO_{2+x} modeled in this work from the non-stoichiometry and electrical conductivity is summarized in Table 2 together with those reported by Matsui and Naito [9,10] and Une and Oguma [13] for comparison.

3.4. Mobility of electron–holes

From Eqs. (10) and (11), the mobility of electron–holes (μ_h) is given in terms of the electrical conductivity and non-stoichiometry as follows:

Table 2
Defect structure of hyper-stoichiometric UO_{2+x} at 1000°C

P_{O_2} region	This work		Matsui and Naito[a] [9,10]		Une and Oguma [8]	
	x, σ	Defect model	x, σ	Defect model	x, σ	Defect model
High P_{O_2}	$x \propto P_{O_2}^{1/2}$	$(2O_i^a 2O_i^b 2V_O)'$	$x \propto P_{O_2}^{1/2}$	$(2O_i^a 2O_i^b 2V_O)'$	$x \propto P_{O_2}^{1/2}$	$(2O_i^a 2O_i^b 2V_O)'$
	$\sigma \propto P_{O_2}^{1/2}$		$\sigma \propto P_{O_2}^{1/2}$		–	
Intermediate P_{O_2}	$x \propto P_{O_2}^{1/5}$	$(2O_i^a 2O_i^b 2V_O)''''$	$x \propto P_{O_2}^{1/12}$	$((2O_i^a 2O_i^b 2V_O)^{5\prime}$	$x \propto P_{O_2}^{1/5}$	$(2O_i^a 2O_i^b 2V_O)''''$
	$\sigma \propto P_{O_2}^{1/5}$		$\sigma \propto P_{O_2}^{1/12}$		–	
Low P_{O_2}			$x \propto P_{O_2}^{1/2}$	$((2O_i^a 2O_i^b 2V_O)^\times$		
			$\sigma \propto P_{O_2}^{1/\infty}$			

[a] The non-stoichiometry and electrical conductivity were measured at 1009°C.

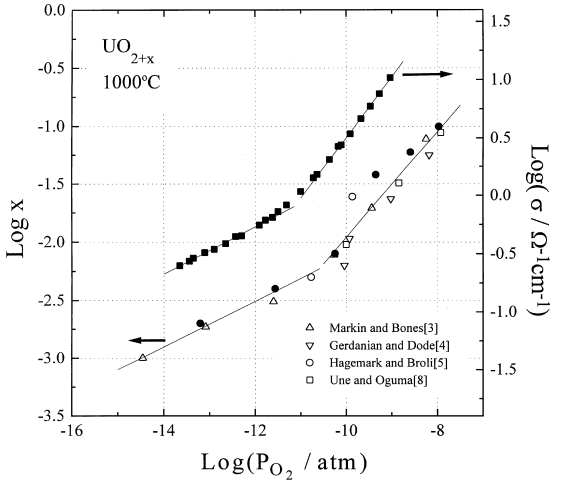

Fig. 5. Non-stoichiometry and electrical conductivity of hyper-stoichiometric UO_{2+x} at 1000°C as a function of oxygen partial pressure (P_{O_2}). Solid circles and squares are the non-stoichiometry and electrical conductivity, respectively, measured in the present work. The solid lines are fitting results for each P_{O_2} region as listed in Table 3.

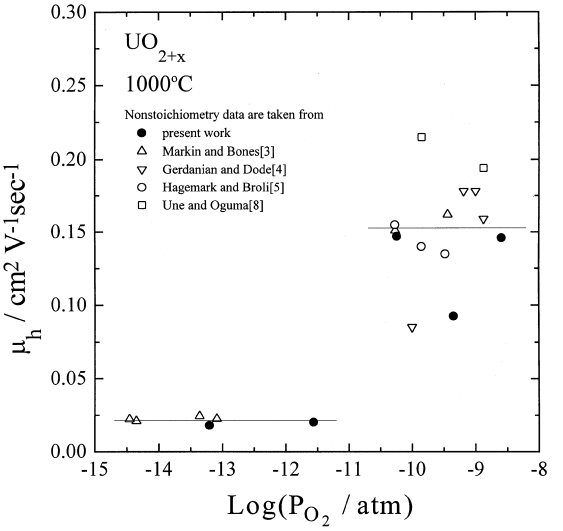

Fig. 6. Mobility of electron-holes of hyper-stoichiometric UO_{2+x} at 1000°C as a function of oxygen partial pressure (P_{O_2}). Solid lines are average values at each P_{O_2} regime.

$$\mu_h = \frac{a_0^3 \sigma}{2nqx}. \tag{12}$$

Then, using the non-stoichiometry and electrical conductivity data, the mobility of electron–holes can be calculated. The non-stoichiometry and electrical conductivity of hyper-stoichiometric UO_{2+x} measured in this work at 1000°C are co-plotted in Fig. 5, where the literature data on the non-stoichiometry exhibiting the same oxygen partial pressure dependence as the present work are also shown. The solid lines in Fig. 5 are the fitting results obtained by linear regression for each P_{O_2} region, which are listed in Table 3. In the evaluation of the mobility with Eq. (12), a_0 for the stoichiometric UO_2 or 5.4707Å [22] was used with the assumption that the change of the lattice constant of UO_{2+x} with non-stoichiometry is negligible. In fact, in the composition range investigated in this work $(0 < x < 0.1)$, the lattice parameter varies by less than 0.2% [23]. The mobility of electron–holes calculated in this way is shown in Fig. 6. At the intermediate P_{O_2} region, the mobility is about 0.02 cm^2/V s, whereas it is about 0.15 cm^2/V s at the high P_{O_2} region with relatively large scattering of data. It is interesting to note that the mobility of the same type of charge carriers (electron–holes in this case), which is in general believed to be constant independent of oxygen partial pressure, shows different values depending on the P_{O_2} regimes. It may arise from different interactions between the defect clusters and holes depending on the charge state of the clusters, lattice distortion due to the oxygen non-stoichiometry, and so on. But the exact explanation cannot be given in this study. Aronson et al. [24] reported the mobility of UO_{2+x} to be 0.055 cm^2/V s at 1100°C from the electrical conductivity and Seebeck coefficient measurements. According to Dudney et al. [11], the mobility of electron–holes of UO_{2+x} doped with 0–10 mol% yttrium at 1000°C and intermediate P_{O_2} region was calculated to be 0.07 cm^2/V s from the electrical conductivity–non-stoichiometry correlation.

4. Summary and conclusions

The non-stoichiometry (x) and electrical conductivity (σ) of hyper-stoichiometric UO_{2+x} were measured at 1000°C as a function of oxygen partial pressure (P_{O_2}) via solid-state coulometric titration and dc 4-probe method,

Table 3
Linear regression results of the non-stoichiometry and electrical conductivity shown in Fig. 5

P_{O_2} region	Non-stoichiometry (x)	Electrical conductivity (σ)
High P_{O_2} region	$\log x = (2.6 \pm 0.4) + (0.46 \pm 0.05)\log(P_{O_2}/\text{atm})$	$\log \sigma = (5.7 \pm 0.1) + (0.52 \pm 0.01)\log (P_{O_2}/\text{atm})$
Intermediate P_{O_2} region	$\log x = -(0.1 \pm 0.2) + (0.20 \pm 0.01)\log(P_{O_2}/\text{atm})$	$\log \sigma = (2.16 \pm 0.05) + (0.202 \pm 0.004)\log (P_{O_2}/\text{atm})$

respectively. Both of the properties exhibited the same P_{O_2}-dependence: $x, \sigma \propto P_{O_2}^{1/2}$ at the high P_{O_2} region and $x, \sigma \propto P_{O_2}^{1/5}$ at the intermediate P_{O_2} region. From the P_{O_2}-dependencies of the non-stoichiometry and electrical conductivity, the defect structure of hyper-stoiciometric UO_{2+x} was analyzed using the Willis $(2O_i^a 2O_i^b 2V_O)$ cluster and it was concluded that the singly ionized $(2O_i^a 2O_i^b 2V_O)'$ cluster is prevailing at the high P_{O_2} region and the quadruply ionized $(2O_i^a 2O_i^b 2V_O)''''$ cluster at the intermediate P_{O_2} region. From the correlation between the non-stoichiometry and electrical conductivity, the mobility of electron–holes was calculated to be about 0.15 and 0.02 cm^2/V s at the high and intermediate P_{O_2} regions, respectively.

Acknowledgements

This project has been carried out under the Nuclear R&D Program by Ministry of Science and Technology in Korea.

References

[1] A. Nakamura, T. Fujino, J. Nucl. Mater. 140 (1986) 113.
[2] Y. Iwano, J. Nucl. Mater. 209 (1994) 79.
[3] T.L. Markin, R.J. Bones, AERE-R4042 and R4178 (1962).
[4] P. Gerdanian, M. Dode, J. Chim. Phys. 62 (1965) 171.
[5] K. Hagemark, M. Broli, J. Inorg. Nucl. Chem. 28 (1966) 2837.
[6] Y. Saito, J. Nucl. Mater. 51 (1974) 112.
[7] M. Ugajin, J. Nucl. Sci. Technol. 20 (1983) 228.
[8] K. Une, M. Oguma, J. Nucl. Mater. 115 (1983) 84.
[9] T. Matsui, K. Naito, J. Nucl. Mater. 132 (1985) 212.
[10] T. Matsui, K. Naito, J. Nucl. Mater. 136 (1985) 59.
[11] N.J. Dudney, R.L. Coble, H.L. Tuller, J. Am. Ceram. Soc. 64 (1981) 627.
[12] T. Ishii, K. Naito, K. Oshima, J. Nucl. Mater. 36 (1970) 288.
[13] H.M. Lee, J. Nucl. Mater. 48 (1973) 107.
[14] S.-H. Kang, H.-I. Yoo, J. Solid State Chem. 139 (1998) 128.
[15] S.-H. Kang, H.-I. Yoo, H.S. Kim, Y.W. Lee, Kor. J. Ceram. Soc. 4 (1998) 78.
[16] H.-I. Yoo, H.L. Tuller, J. Am. Ceram. Soc. 70 (1987) 388.
[17] H.-I. Yoo, H.L. Tuller, J. Mater. Res. 3 (1988) 552.
[18] J.-H. Kim, H.-I. Yoo, H.L. Tuller, J. Am. Ceram. Soc. 73 (1990) 258.
[19] B.T.M. Willis, Acta Crystallogr. A34 (1978) 88.
[20] H.S. Kim, Y.K. Yoon, Y.W. Lee, J. Nucl. Mater. 226 (1995) 206.
[21] A. Nakamura, T. Fujino, J. Nucl. Mater. 149 (1987) 80.
[22] D.I.R. Norris, P. Kay, J. Nucl. Mater. 116 (1983) 184.
[23] D.A. Vaughan, Uranium Dioxide: Properties and Nuclear Applications, in: J. Belle (Ed.), Nuclear-Chemie Metallurgie G.m.b.H, Division of Reactor Development, United States Atomic Energy Commission, 1961, p. 174.
[24] S. Aronson, J.E. Rulli, B.E. Schaner, J. Chem. Phys. 35 (1961) 1382.